Inorganic Chemistry

pubs.acs.org/IC

Article

Thiol, His−His Motif, and the Battle over Cu(II) in the Relationship of CopM Metallophore and OprC Outer Membrane Protein

Aleksandra Hecel,* Arian Kola, Daniela Valensin, and Danuta Witkowska

Cite This: *Inorg. Chem.* 2025, 64, 2936−2950

Read Online

ACCESS | Metrics & More | Article Recommendations | Supporting Information

ABSTRACT: The mechanisms of Cu import across the bacterial outer membrane have been investigated only in a few cases. One such mechanism involves the outer membrane OprC transporter with a unique CxxxM-HxM metal-binding site, discovered recently. This newly identified site in OprC is located outside the cell and is, therefore, most likely to bind Cu(II) through this domain. Since OprC may interact with azurin to facilitate the removal of copper, our study investigated the potential role of CopM metallophore. We selected two putative metal-binding sites in CopM, characterized by MxxHH and MHxxH motifs, which can bind Cu(II) and may interact with the extracellular CxxxM-HxM motif of OprC. At pH 7, the MxxHH motif in CopM was the most effective ligand for Cu(II) ions compared to the MHxxH domain and the novel CxxxM-HxM site in OprC. Furthermore, the CxxxM-HxM site in OprC, where a cysteine residue also binds Cu(II) ions alongside histidine, does not effectively compete with the MxxHH metal-binding site in CopM. This comparison suggests that the CopM MxxHH domain binds Cu(II) ions very strongly and is unable to give them back to the OprC; therefore, it is perhaps transported together with copper ions through OprC into the bacterial cell.

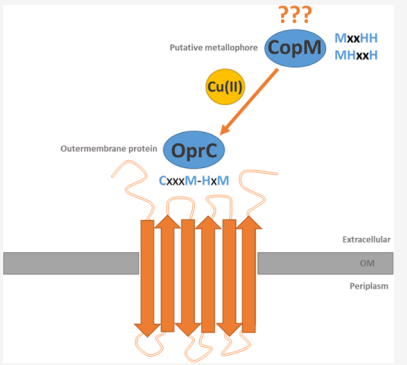

INTRODUCTION

There is a significant gap in understanding copper import systems in prokaryotic organisms. Although the Ctr family transporters are quite well-described, the bacterial copper influx mechanism is very poorly understood, primarily because bacterial copper proteins tend to localize in the periplasmic and extracellular space.[1,2] Furthermore, bacterial Cu transport systems are far more diverse than those in eukaryotes, and some copper uptake mechanisms are confined to one bacterial group or even one species; hence, understanding the transport mechanism is extremely complex. Studies on bacterial copper transport have mainly focused on copper export (in order to detoxify the microbial cell), while the mechanisms of copper import across the outer membrane of Gram-negative bacteria and the bacterial cytoplasmic membrane have been examined in only a few cases.[3,4]

Microorganisms are aware of the importance of the acquisition of substantial metal trace elements. Transition metals are significant for the survival of all organisms, being crucial for metalloproteins, such as metalloenzymes, storage proteins, and transcription factors. Pathogens have developed highly efficient transport systems, which rely on (i) chaperones, metal-chelating molecules present in microorganisms in order to efficiently bind metal ions and (ii) transmembrane transporters (importer and exporter) that interact with specific chaperones and are capable of transporting metal ions into the periplasm and cytoplasm. The effective acquisition of metal ions is often considered as a virulence factor and is thus a potential target for novel antimicrobial therapies.[5] In general, the copper transport system in Gram-negative bacteria is more complex than that in Gram-positive ones due to the presence of the periplasmic space. It includes (i) transmembrane proteins, which are responsible for capturing and transporting copper ions to or from the periplasm and cytosol (e.g., CcoA, OprC, CuiT, CopA, CusABC) and (ii) peptide chaperones in the periplasmic and cytoplasmic space (e.g., PcoC, CopZ, CusF), whose role is to deliver copper to specific importer/exporter anchored in the membrane and/or deliver copper ions to other proteins (e.g., enzymes).[6,7] This very complex system is also completed by sensors regulating the bioavailability of Cu(I) in the cell compartment and storage copper proteins. Depending on whether a given transporter is localized outside or inside the cell, it can bind copper ions in different oxidation states.

Only few copper influx proteins have been identified in bacteria so far—the outer membrane, OprC, and the inner-membrane transporters, CcoA[8] and CuiT.[9] OprC (*P00282, UniProt*) is an outer membrane, TonB-dependent transporter that is conserved in many *Proteobacteria* and which mediates acquisition of both reduced and oxidized ionic copper.[10−13] It binds Cu(II)/Cu(I) via an unprecedented CxxxM-HxM metal-binding site, discovered recently.[12] Furthermore, the blue

Received: November 28, 2024
Revised: January 25, 2025
Accepted: January 31, 2025
Published: February 6, 2025

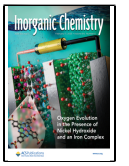

copper protein azurin was reported to be secreted by *Pseudomonas aeruginosa* and to interact with OprC, suggesting a role of the latter in Cu(II) uptake. There is not much information in the literature about copper-binding peptide metallophores identified in bacteria. The copper resistance system in the cyanobacterium *Synechocystis* comprises two operons, previously described copBAC, which are expressed in response to copper in the media, and copMRS, which codes for a protein of unknown function. One of them is CopM (*A0A0F6QDN6, UniProt)* protein, which is able to bind both Cu(I) and Cu(II).[14,15] It is worth noting that CopM was localized not only in the periplasm but also in the extracellular space. It suggests that CopM can act not only as chaperone but also as a metallophore, excreting outside the pathogen in order to efficiently bind copper ions. This can serve either as metal acquisition or as a way of protecting the atoms against the toxic excess of metal ions. CopM involves a DUF305 domain of unknown function with a characteristic $_{53}$MxxHH$_{57}$ motif, located in the first α-helical domain.[16] The Cu(II)−CopM structure from crystals soaked with Cu(II) was determined, and residues 114−125 of the linker region can be traced in the electron-density map. In this region, two histidine residues may constitute the copper-binding site, with the $_{117}$MHxxH$_{121}$ motif.[15]

In this study, we focus on Cu(II) complexes involving a novel CxxxM-HxM metal-binding site from an OprC transmembrane protein. This newly identified OprC site is localized outside the cell, and therefore, it is most likely to bind Cu(II) through this domain. The Ac-$_{141}$GA**C**PNR**M**DA$_{149}$AAAAAA$_{321}$AD**HIM**D$_{326}$-NH$_2$ sequence was synthesized with two binding domains connected with a 6Ala linker. Due to the fact that OprC may interact with azurin to effectively withdraw copper ions, our study also focused on the potential CopM metallophore. We have chosen two putative Cu(II) binding sites from the CopM amino acid sequence (Ac-$_{51}$EM**M**TP**HH**QDAIDMAEMALQKAEHPE$_{75}$-NH$_2$ and Ac-$_{113}$GMMG**MH**QG**H**GMMAMD$_{127}$-NH$_2$), which contain MxxHH and MHxxM motifs, respectively, capable of binding Cu(II) and can possibly interact with the extracellular CxxxM-HxM OprC domain to convey a metal ion into the bacterial cell. Potentiometric titrations were used to calculate the thermodynamic parameters of the investigated systems. We determined the partial and overall stability constants for all formed Cu(II) complexes. In order to precisely establish metal-binding sites, donor atoms involved in the coordination sphere, and the coordination geometry of the formed complexes, several spectroscopic techniques—UV−vis, circular dichroism (CD), NMR and electron paramagnetic resonance (EPR) measurements—were registered at different pH values.

EXPERIMENTAL SECTION

Materials. Three peptides, Ac-GA**C**PNR**M**DAAAAAAAAD-**HIM**D-NH$_2$, Ac-EM**M**TP**HH**QDAIDMAEMALQKAEHPE-NH$_2$, and Ac-GMMG**MH**QG**H**GMMAMD-NH$_2$, were purchased from Karebay Biochem, with a certified purity of 98%, and used as received. Cu(II) perchlorate, obtained from Sigma-Aldrich, was of extra pure grade. A carbonate-free stock solution of 0.1 M KOH was also purchased from Sigma-Aldrich and subsequently standardized potentiometrically using potassium hydrogen phthalate.

Potentiometric Measurements. The stability constants for proton and Cu(II) complexes with three ligands were determined from titration curves obtained over a pH range of 2−11, at 298 K and at an ionic strength of 0.1 M $NaClO_4$. Each titration used a total solution volume of 3.0 cm^3. The potentiometric titrations were conducted using a Dosimat 800 Metrohm Titrator paired with a Metrohm 905 pH meter and a Mettler Toledo pH InLab Science electrode. The titration setup included a thermostabilized glass cell with magnetic stirring, a microburet delivery tube, and an argon inlet−outlet tube. Titrations were performed with 0.1 M carbonate-free NaOH. Daily calibration of the electrodes for hydrogen ion concentration was achieved by titrating $HClO_4$ with NaOH in a 3.0 cm^3 solution. Ligand concentrations were maintained at 0.4 and 0.5 mM, with metal-to-ligand ratios at 1:1. The concentrations and purities of the ligand solutions were verified by using the Gran method. The standard potential and electrode slope were calculated using the GLEE program.[17] Stability constants were calculated with the HYPERQUAD 2008 software[18] and speciation diagrams were generated using the HYSS program.[19]

Spectroscopic Studies. Absorption spectra were recorded using a Jasco-730 spectrophotometer over the range 200−800 nm, with a 1 cm optical path length quartz cuvette. Circular dichroism (CD) spectra were measured on a Jasco J-1500 CD spectrometer within the 200−800 nm range, utilizing a quartz cuvette with a 1 cm and 0.01 mm optical path for the visible and near-UV range. The sample solution concentrations used in the spectroscopic studies were consistent with those used in the potentiometric experiments, maintaining a metal-to-ligand ratio of 1:1. All spectroscopic measurements were recorded in the pH range 3−11. The pH of the samples was adjusted with the appropriate amounts of $HClO_4$ and NaOH solutions. The UV−vis and CD spectroscopy parameters were calculated from the spectra obtained at pH values corresponding to the maximum concentration of each particular species based on distribution diagrams. The spectra were processed and visualized using OriginPro 2016. Electron paramagnetic resonance (EPR) spectra were recorded in liquid nitrogen on a Bruker ELEXSYS E500 CW-EPR spectrometer at X-band frequency (frequency = 9.5 GHz, modulation amplitude = 10.00 G) and equipped with an ER 036TM NMR teslameter and an E41 FC frequency counter. Ethylene glycol (25%) was used as a cryoprotectant. Ligand concentration was 1 mM and Cu(II)-to-ligand ratio = 1:1. The EPR parameters were analyzed by simulating the experimental spectra using WIN-EPR SIMFONIA software, version 1.2 (Bruker).

Mass Spectrometry. High-resolution mass spectra were acquired by using a Bruker compact QTOF mass spectrometer (Bruker Daltonik, Bremen, Germany) with an electrospray ionization source featuring an ion funnel. The instrument operated in positive ion mode with the following settings: scan range of m/z 100−2000, nitrogen as the dry gas, a temperature of 453 K, and ion energy of 5 eV. The capillary voltage, optimized for the highest signal-to-noise ratio, was set at 4800 V. Samples were prepared in a 1:1 methanol-to-water mixture (MeOH) at pH 6−7, with a metal-to-ligand molar ratio of 1:1 and a total ligand concentration of 0.1 mM. Infusion was carried out at a flow rate of 3 μL/min. External calibration of the instrument was performed using a Tunemix mixture (Bruker Daltonik, Germany) with quadratic regression. Data analysis was conducted with Compass DataAnalysis 4.2 software (Bruker Daltonik, Germany). Calibration accuracy was better than 5 ppm, allowing for unambiguous confirmation of the elemental composition of the complex using the true isotopic pattern and SigmaFit.

NMR. All NMR experiments were conducted at a magnetic field strength of 14.1 T using a Bruker Avance III 600 MHz spectrometer, with the temperature maintained at 288 K. A 5 mm broadband inverse (BBI) probe was employed for all measurements. The residual water signal was suppressed through excitation sculpting, utilizing a selective square pulse of 2 ms duration targeting water.[20] A typical NMR spectrum was recorded with 16 transients, a spectral width of 7200 Hz, and a recycle delay of 2.0 s. Proton resonance assignments for all of the peptide sequences were made using two-dimensional (2D) ^{1}H−^{1}H TOCSY and NOESY experiments. The TOCSY experiment was performed with a 60 ms spin-locking period by using the MLEV-17 mixing sequence. NOESY spectra were acquired at various mixing times to optimize the conditions. Data processing was completed using TopSpin v 3.6 software.

https://doi.org/10.1021/acs.inorgchem.4c05101
Inorg. Chem. 2025, 64, 2936−2950

Isothermal Titration Calorimetry (ITC). Isothermal titration calorimetry (ITC) experiments were conducted at 25 °C using a MicroCal PEAQ titration calorimeter from Malvern, U.K. All reagents were of high purity (>99%) and obtained from Sigma-Aldrich. The peptides were dissolved directly in sodium cacodylate (Caco) buffer solution, pH 7.0. A metal stock solution of copper(II) ions was prepared at a concentration of 100 mM in deionized water (18 MΩ) at a low pH (~2). Working solutions of copper(II) ions (1−2 mM) in Caco buffer were then prepared by dilution, with the pH adjusted to 7.0 using either NaOH or HCl.

Prior to titration, the instrument was stabilized at 25 °C. A total of 40 μL of the metal-buffer solution (1−2 mM) was used to titrate 200 μL of the peptide buffer solution, which initially had a concentration 10 times lower than that of the metal ion. Each assay was repeated at least three times. Each titration comprised 19 successive injections, with intervals of 180−240 s between each aliquot (depending on the time required for complete equilibration) and a stirring speed of 750 rpm.[21] Additionally, a competitive reaction was conducted in which the Ac-EM**M**TP**HH**QDAIDMAEMALQKAEHPE-NH_2 peptide (at a concentration of 1 mM) was titrated into the Ac-GA**C**PNR**M**-DAAAAAAAAD**HIM**D-NH_2 peptide (0.1 mM) that was already bound to copper ions, maintaining a 1:1 ratio.

The heat of dilution from an analogous control titration was subtracted prior to data fitting, and an initial injection of 0.4 μL was discarded from each data set to negate the effect of titrant diffusion across the syringe tip during the equilibration phase. Periodic titrations with $CaCl_2$−EDTA were performed for comparison with the results obtained during the initial calibration of the instrument. Data analysis was performed using MicroCal PEAQ-ITC Analysis Software. The one-site binding model yielded the best-fit values for stoichiometry (N), enthalpy change (ΔH), and equilibrium constant (K_d).

RESULTS AND DISCUSSION

Ligand Protonation Constants of OprC and CopM. All peptides are protected in the N-terminus through acetylation and in the C-terminus through amidation.

The OprC fragment Ac-GA**C**PNR**M**DAAAAAAAAD-**HIM**D-NH_2 contains three Asp residues, which can release a proton from their carboxylic side chain. In addition to these acidic residues, the peptide has one histidine and one cysteine residue, which participate in acid−base equilibria through the imidazole ring and thiol group of their side chains, respectively (Table 1A). The release of acidic protons from Asp residues occurs with a dissociation constant of 2.53−4.46. The pK_a values of the side imidazole group of histidine (6.92) and thiol group of cysteine (9.56) are in agreement with literature values. For the metal-binding domain of CopM with the $_{53}$MxxHH$_{57}$ motif, Ac-EM**M**TP**HH**QDAIDMAEMALQ-KAEHPE-NH_2, 11 protonation constants were detected (Table 1B). The six lowest constants (pK_a = 3.11−5.14) correspond to deprotonation of the carboxylic group of aspartic and glutamic acid residues. According to the literature,[22] the two lower values were assigned to aspartic acid, which is generally more acidic than glutamic acid. The next three deprotonation constants (pK_a = 6.18, 6.86, and 7.43) can be assigned to the three imidazole groups from side chains of histidine residues. The highest pK_a = 9.94 belongs to the ε amine group of side chains of the lysine residue.

For the CopM fragment, which contains the $_{117}$MHxxH$_{121}$ motif, Ac-GMMG**MH**QG**H**GMMAMD-NH_2, 3 groups are involved in acid−base reactions: the aspartic acid side chain carboxylate and two histidine imidazoles with pK_a values 3.80, 5.95, and 7.01, respectively (Table 1C). All of the obtained protonation constants log β and calculated pK_a values for three ligands are in good agreement with the literature data for similar peptide systems.[23−26]

Table 1. Protonation Constants for (A) Ac-GACPNRMDAAAAAAAADHIMD-NH_2, (B) Ac-EMMTPHHQDAIDMAEMALQKAEHPE-NH_2, and (C) Ac-GMMGMHQGHGMMAMD-NH_2, T = 298 K, I = 0.1 M ($NaClO_4$)[a]

	log β_{jk}[b]	pK_a[c]	aa
(A) Ac-GACPNRMDAAAAAAAADHIMD-NH_2			
$[H_5L]^{+}$	27.02(3)	2.53	D
$[H_4L]$	24.49(3)	3.55	D
$[H_3L]^{-}$	20.94(3)	4.46	D
$[H_2L]^{2-}$	16.48(3)	6.92	H
$[HL]^{3-}$	9.56(3)	9.56	C
(B) Ac-EMMTPHHQDAIDMAEMALQKAEHPE-NH_2			
$[H_{10}L]^{4+}$	55.35(6)	3.11	D
$[H_9L]^{3+}$	52.24(4)	3.58	D
$[H_8L]^{2+}$	48.66(3)	4.04	E
$[H_7L]^{+}$	44.62(3)	4.34	E
$[H_6L]$	40.28(3)	4.73	E
$[H_5L]^{-}$	35.55(2)	5.14	E
$[H_4L]^{2-}$	30.41(2)	6.18	H
$[H_3L]^{3-}$	24.23(2)	6.86	H
$[H_2L]^{4-}$	17.37(2)	7.43	H
$[HL]^{5-}$	9.94(1)	9.94	K
(C) Ac-GMMGMHQGHGMMAMD-NH_2			
$[H_3L]^{2+}$	16.76(2)	3.80	D
$[H_2L]^{+}$	12.96(2)	5.95	H
$[HL]$	7.01(2)	7.01	H

[a]Values in parentheses are standard deviations of the last significant figure. [b]Constants are presented as cumulative log β_{jk} values. $\beta(H_jL_k) = [H_jL_k]/([H]_j[L]_k)$, in which $[L]$ is the concentration of the fully deprotonated peptide. [c]pK_a values of the peptides were derived from cumulative constants: pK_a = log $\beta(H_jL_k)$ − log $\beta(H_j - 1L_k)$.

OprC and CopM Copper(II) Complexes. The structural and thermodynamic properties of OprC and CopM-fragment copper complexes (the M/L stoichiometric ratio of 1:1) were studied using mass spectrometry, potentiometry, UV−vis, CD, NMR spectroscopy, and ITC.

Mass spectrometry revealed the stoichiometry of the copper complexes, showing that under the discussed conditions, only monometallic 1:1 Cu/L species exist in the solution for three systems. The MS spectra (Figure S1) and table (Table S1) with m/z values for three peptides and their copper complexes are presented in the Supporting Information. The m/z signals of free ligands and their Cu(II) complexes were confirmed by the analysis of the isotopic distribution of their signals and by the comparison of the experimental signals with those of their simulations.

In the case of the **Cu(II)-Ac-GACPNRMDAAAAAAAAD-HIMD-NH_2** OprC fragment complex, six mononuclear species exist in the studied pH values (Figure 1A). The first formed species is $[CuH_2L]$, in which three carboxylic groups from aspartic acid are deprotonated and can participate in Cu(II) binding at low pH. The next form, $[CuHL]^{-}$, results from the deprotonation of a His imidazole nitrogen. The lower pK_a value compared to free ligand provide $1N_{im}$ binding mode suggesting that the residue is involved in Cu(II) binding (Table 2A). Moreover, the d−d band at 715 nm with ε = 13.0 M^{-1} cm^{-1} (Figure 1B and Table 2A) and EPR parameters A_{II} = 150 G and g_{II} = 2.33 (Figure S2A and Table 2A) strongly

https://doi.org/10.1021/acs.inorgchem.4c05101
Inorg. Chem. 2025, 64, 2936−2950

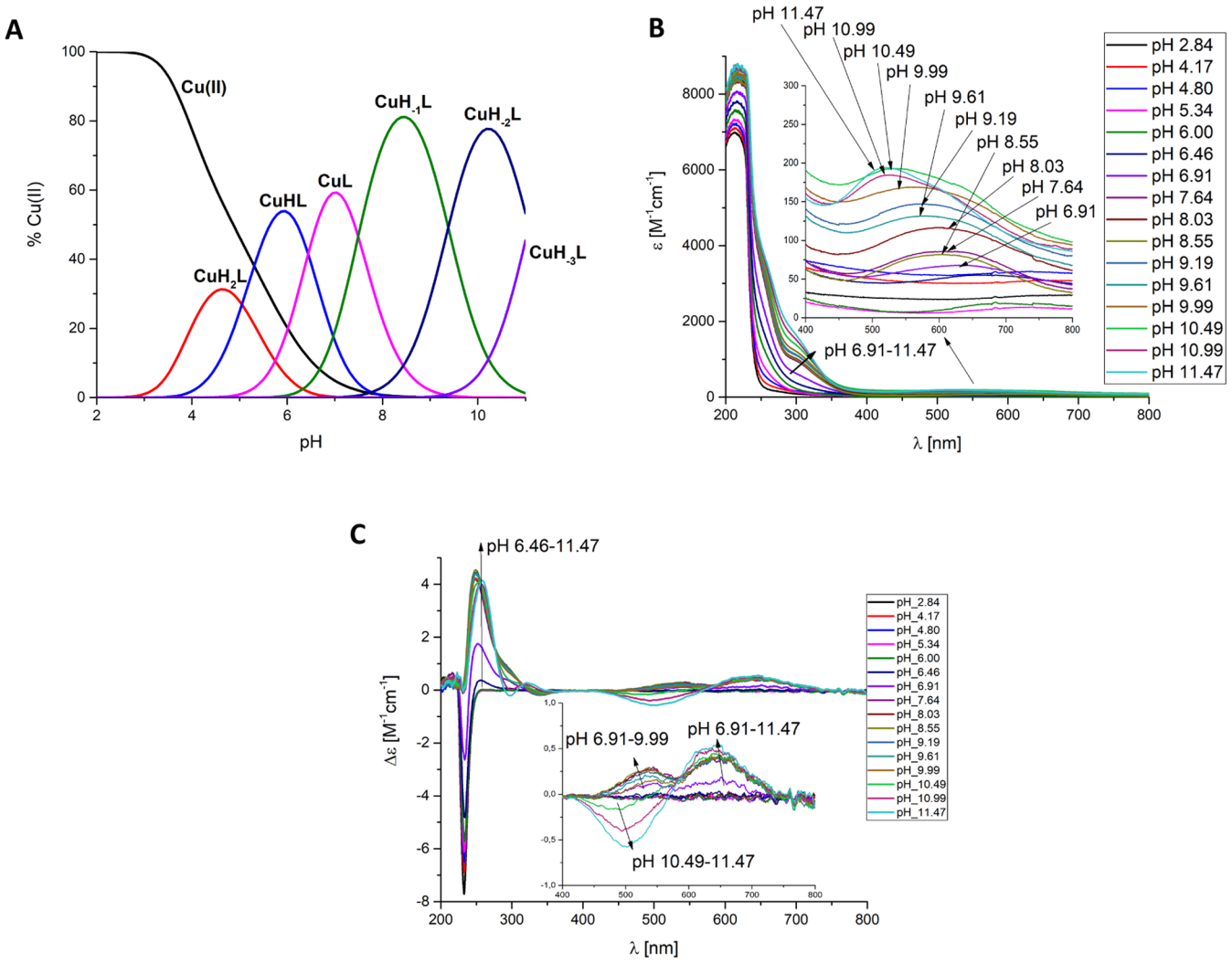

Figure 1. (A) Species distribution diagram, (B) UV−vis absorption spectra, and (C) CD spectra of Cu(II)-Ac-GACPNRMDAAAAAAAADHIMD-NH_2; metal/ligand ratio 1:1; $C_L = 5 \times 10^{-4}$ M. For clarity, the charges on the speciation plot were omitted (see Table 2A).

support the presence of 1 nitrogen atom in the coordination sphere.[23,27,28] The CuL species, with maximum concentration at pH 7, results from the deprotonation and Cu(II) binding to the first amide nitrogen from the peptide backbone. The 2N binding for $[CuL]^{2-}$ species is confirmed by a d−d band at 633 nm with ε = 48.5 M^{-1} cm^{-1} (Figure 1B and Table 2A).[29] The $[CuH_{-1}L]^{3-}$ species, with a maximum concentration at pH 8.5, may result from the deprotonation and Cu(II) binding to the Cys thiol group. The presence of a band at around 330 nm may prove S_{Cys}-Cu(II) charge transfer and involvement of the cysteine sulfur in binding (Figure 1B,C).[30,31] The lowered cysteine pK_a value in the complex in relation to the free ligand (pK_a 9.56 (ligand) → pK_a 7.49 (complex)) strongly suggests that the cysteine residue is involved in the Cu(II) ion coordination. Additionally, on the CD spectra, two positive bands at 537 and 647 nm indicate the Cu(II)-amide binding with a slight tendency to form square-planar geometry with a $1N_{im}$, $1N^-$, and $1S^-$ binding mode (Figure 1C). The involvement of two nitrogen atoms in Cu(II) binding is confirmed by UV−vis (d−d band at 603 nm with ε = 58.4 M^{-1} cm^{-1}) and EPR parameters (A_{II} = 160 G and g_{II} = 2.24) (Figures 1B, S2A and Table 2A). The loss of the next proton leads to the $[CuH_{-2}L]^{4-}$ complex species, with a maximum concentration at pH 10. At this pH, a hypsochromic effect is observed in the UV−vis spectra, from 603 to 570 nm, and EPR parameters (A_{II} = 170 G and g_{II} = 2.22) suggest a 3N coordination mode with a $1N_{im}$, $2N^-$, and $1S^-$ donor set (Table 2A, Figures 1B and S2A). The presence of a typical negative (λ = 502 nm, $\Delta\varepsilon$ = −0.57 cm^{-1} M^{-1}) and positive (λ = 646 nm, $\Delta\varepsilon$ = 0.56 cm^{-1} M^{-1}) Cotton effect for the last $[CuH_{-3}L]^{5-}$ species suggests the formation of a square-planar complex (Figure 1C and Table 2A).[32,33] The involvement of four nitrogen atoms $1N_{im}$, $3N^-$ in the binding is confirmed by the blue shift of the d−d band from 570 to 521 nm in UV−vis spectra (Figure 1B and Table 2A).[34,35] To this species, the $1N_{im}$, $3N^-$ binding mode was assigned. At pH 10.5−11, a flattening of the band at 330 nm was also observed (Figure 1B), suggesting displacement of the cysteinyl residue by the coordinating third amide.

It is worth noticing that all analyzed peptide domains also contain methionyl residues in their sequences. Due to the lack of deprotonating side chains in the methionyl residue ($-SCH_3$ group), the participation of thioether groups in the binding of Cu(II) ions cannot be confirmed or excluded using potentiometric titrations. Also, UV−vis spectroscopy will not tell us more about Met−Cu(II) interactions. The existence of a CT band on UV−vis spectra around 320−330 nm was assigned to S(thioether) → Cu(II) interactions in the

https://doi.org/10.1021/acs.inorgchem.4c05101
Inorg. Chem. 2025, 64, 2936−2950

Table 2. Stability Constants, Spectroscopic Parameters, and Proposed Coordination Modes for Cu(II) Complexes with (A) Ac-GACPNRMDAAAAAAAADHIMD-NH_2, (B) Ac-EMMTPHHQDAIDMAEMALQKAEHPE-NH_2, and (C) Ac-GMMGMHQGHGMMAMD-NH_2 at T = 298 K[a]

			UV		CD		EPR		
	$\log \beta_{ijk}$[b]	pK_a[c]	λ [nm]	ε [cm^{-1} M^{-1}]	λ [nm]	$\Delta\varepsilon$ [cm^{-1} M^{-1}]	A_{II}	g_{II}	donors
(A) Cu(II)-Ac-GACPNRMDAAAAAAAADHIMD-NH_2									
$[CuH_2L]$	19.71(6)								
$[CuHL]^-$	14.66(4)	5.05	715	13.0			150	2.33	$1N_{im}$
$[CuL]^{2-}$	8.22(4)	6.44	633	48.5	253	1.76	160	2.28	$1N_{im}$, $1N^-$
					340	−0.11			
					545	0.12			
					650	0.19			
$[CuH_{-1}L]^{3-}$	0.73(5)	7.49	603	58.4	249	4.55	160	2.24	$1N_{im}$, $1N^-$, $1S_{Cys}^-$
			330	537	342	−0.19			
					537	0.29			
					647	0.41			
$[CuH_{-2}L]^{4-}$	−8.65(7)	9.38	570	169	249	4.24	170	2.22	$1N_{im}$, $2N^-$, $1S_{Cys}^-$
			330	704	343	−0.14			
					543	0.15			
					649	0.43			
$[CuH_{-3}L]^{5-}$	−19.72(9)	11.07	521	194	258	4.15	185	2.20	$1N_{im}$, $3N^-$
					300	−0.20			
					321	0.27			
					502	−0.57			
					646	0.56			
(B) Cu(II)-Ac-EMMTPHHQDAIDMAEMALQKAEHPE-NH_2									
$[CuH_5L]^+$	41.74(3)						135	2.36	
$[CuH_3L]^-$	32.82(3)		719	46.7					$1N_{im}$
$[CuH_2L]^{2-}$	27.80(7)	5.02	687	56.4			170	2.29	$2N_{im}$
$[CuHL]^{3-}$	22.65(5)	5.15	678	67.9					$2N_{im}$
$[CuL]^{4-}$	17.02(4)	5.63	647	79.7			180	2.27	$2N_{im}$
$[CuH_{-1}L]^{5-}$	10.29(5)	6.73	615	92.5	261	1.18	185	2.25	$2N_{im}$, $1N^-$
					534	0.33			
$[CuH_{-2}L]^{6-}$	2.51(5)	7.78	593	110	263	3.36	185	2.25	$1N_{im}$, $2N^-$
					534	0.41			
$[CuH_{-3}L]^{7-}$	−5.72(5)	8.23	512	122	264	3.79	195	2.23	$1N_{im}$, $3N^-$
					323	0.25			
					477	−0.52			
					622	0.59			
$[CuH_{-4}L]^{8-}$	−15.28(5)	9.56	509	123	264	3.66	200	2.23	$1N_{im}$, $3N^-$
					320	0.54			
					488	−1.03			
					618	0.96			
(C) Cu(II)-Ac-GMMGMHQGHGMMAMD-NH_2									
$[CuH_2L]^{3+}$	16.76(5)								
$[CuHL]^{2+}$	12.32(4)	4.44	701	82.1	253	0.27			$1N_{im}$
$[CuL]^+$	7.15(4)	5.17	639	119	252	1.28			$2N_{im}$
$[CuH_{-1}L]$	0.40(5)	6.75	574	160	247	2.76			$2N_{im}$, $1N^-$
					314	−0.66			
					518	0.56			
$[CuH_{-2}L]^-$	−6.37(5)	6.77	554	173	242	2.87			$2N_{im}$, $2N^-$
					273	1.78			
					312	−1.17			
					515	0.95			
					605	−0.18			
$[CuH_{-3}L]^{2-}$	−14.41(5)	8.04	532	191	230	3.35			$1N_{im}$, $3N^-$
					275	1.11			
					312	−1.24			
					512	0.96			
					600	−0.46			

https://doi.org/10.1021/acs.inorgchem.4c05101
Inorg. Chem. 2025, 64, 2936−2950

Table 2. continued

[a]Values in parentheses are standard deviations on the last significant figure. [b]Cu(II) stability constants are presented as cumulative log β_{ijk} values. *L* stands for a fully deprotonated peptide ligand that binds Cu(II) ions: $\beta(M_iH_jL_k) = [M_iH_jL_k]/([M]_i[H]_j[L]_k)$, where $[L]$ is the concentration of the fully deprotonated peptide. [c]$pK_a = \log\beta\ (M_iH_j + 1L_k) - \log\beta(M_iH_jL_k)$.

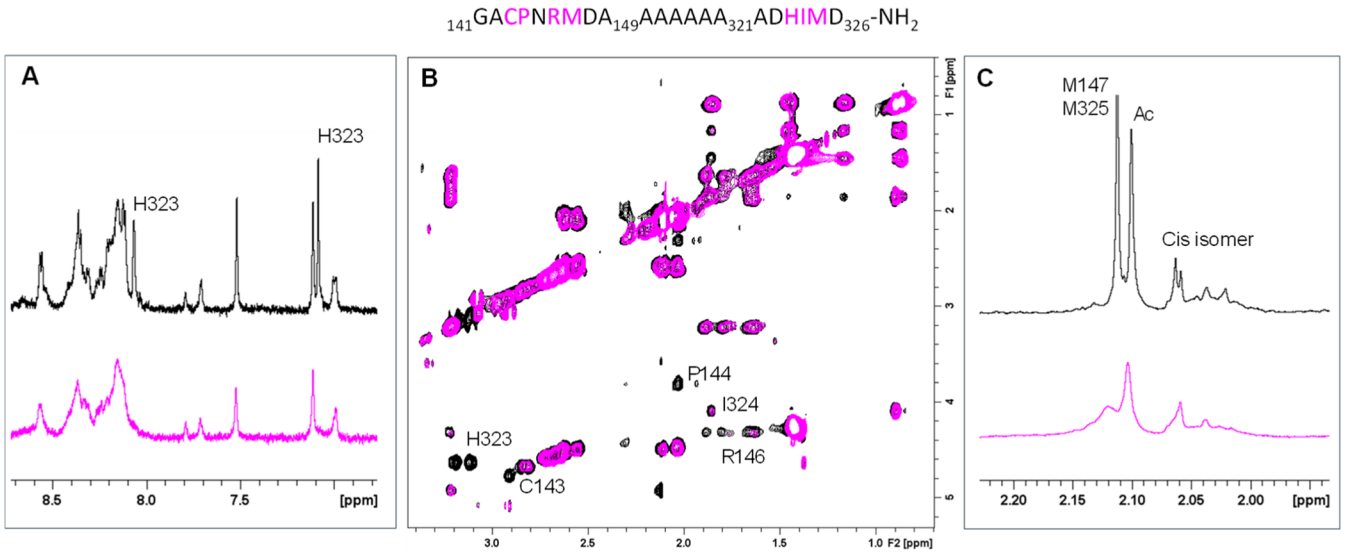

Figure 2. Superimposition of NMR spectra of Ac-$_{141}$GACPNRMDA$_{149}$(AAAAAA)$_{321}$ADHIMD$_{326}$-NH$_2$ (0.5 mM) in the absence (black) and presence (magenta) of 0.2 Cu(II) equivalents. (A) 1D ^{1}H amide and aromatic region, (B) 2D ^{1}H−^{1}H TOCSY aliphatic region, and (C) 1D ^{1}H aliphatic region. Spectra were recorded at 288 K in 20 mM phosphate buffer, pH 7.4. The peptide sequence is shown at the top with the most affected residues highlighted in magenta.

literature, but this was analyzed for tripeptides MGG, GMG, and GGM only.[36] For our systems, where the bands in the range 200−370 nm can be assigned to $n \rightarrow \pi^*/\pi \rightarrow \pi^*$ intraligand transitions associated to other amino acid present in the sequences,[37] specific S(Met) → Cu(II) bands are very likely to be overlapped. Moreover, in this UV region, strong $n \rightarrow \pi^*$ and $\pi \rightarrow \pi^*$ peptide backbone transitions are also present.[38] Thus, the influence of thioether groups of methionyl in the Cu(II) coordination had to be confirmed by using NMR spectroscopy.

Cu(II) to the **Ac-$_{141}$GACPNRMDA$_{149}$(AAAAAA)$_{321}$ADHIMD$_{326}$-NH$_2$** OprC system was investigated using NMR spectroscopy. NMR spectra of the peptide, both in the presence and absence of the metal ion, were recorded at 288 K to monitor the signals of NH protons, which appeared very broad at room temperature, as expected for disordered peptides. All NMR spectra were acquired for peptide solutions in phosphate buffer (pH 7.4) to avoid any shifts due to subtle pH changes. The addition of substoichiometric amounts of Cu(II) (0.2 eqs.) led to selective line broadening of NMR resonances belonging to residues near the metal center. This broadening arises from dipolar coupling between the copper's unpaired electron and the nuclei in close proximity to the metal-binding site.[39−42] Figure 2 shows selected regions of the one-dimensional (1D) and 2D NMR spectra, highlighting the most affected amino acids, including Cys143, His323, and nearby residues, such as Pro144 and Ile324. Additionally, the methyl protons of both methionine residues are significantly impacted by the presence of the paramagnetic ion. The proximity of Met145 to the copper coordination sphere is further supported by the effects observed on Arg146, whose scalar correlations, visible in the TOCSY spectrum, completely disappeared upon the addition of the copper ion. Finally, the analysis of the fingerprint region of the TOCSY spectrum confirmed the previously observed effects on His323 and Ile324, along with a slight variation on Met325 (data not shown). The data indicate copper binding to Cys143 and His323, with the possible involvement of the Met-SCH_3 groups in the metal coordination sphere.

In the Cu(II) binding site of the bacterial metallophore CopM with a characteristic MxxHH motif, **Ac-EMMTPHHQ-DAIDMAEMALQKAEHPE-NH$_2$**, nine Cu(II) complexes were detected (Figure 3A and Table 2B). The first complex detected by potentiometry is $[CuH_5L]^+$ with a maximum at around pH 3.9. The stoichiometry of this species indicates that five acid−base sites are already deprotonated: three Glu and two Asp residues have lost a proton. At this point, most probably, Cu(II) is anchored by carboxyl groups of acidic amino acids.[43−45] The first spectroscopically detectable species is $[CuH_3L]^-$, with a maximal concentration at pH 4.7 where one histidine imidazole should be bound to the copper(II) ion (λ = 719 nm, ε = 46.7 cm^{-1} M^{-1}) (Figure 3B and Table 2B). The next deprotonation step (pK_a = 5.02) for the $[CuH_2L]^{2-}$ species led to the formation of a $2N_{im}$ complex, as indicated by spectroscopic UV−vis and EPR parameters (λ = 687 nm, ε = 56.4 cm^{-1} M^{-1}, g_{II} = 2. 29, A_{II} = 170) (Figures 2B and S2B). For the next two species, $[CuHL]^{3-}$ and $[CuL]^{4-}$, no significant shifts in the UV−vis spectra are observed, indicating no changes in the 2N binding mode. The calculated pK_a values, 5.15 for $[CuHL]^{3-}$, could result from the deprotonation of an unbound histidine residue (Table 2B). The observed decrease of the pK_a value for the third histidine (5.15) in the $[CuHL]^{3-}$ species compared to the free ligand $[H_2L]^{4-}$ (7.43) suggests that Cu(II) can coordinate to all imidazoles present in the sequence but only to two at the same time. The pK_a value (5.63) for $[CuL]^{4-}$ species cannot be assigned to the

https://doi.org/10.1021/acs.inorgchem.4c05101
Inorg. Chem. 2025, 64, 2936−2950

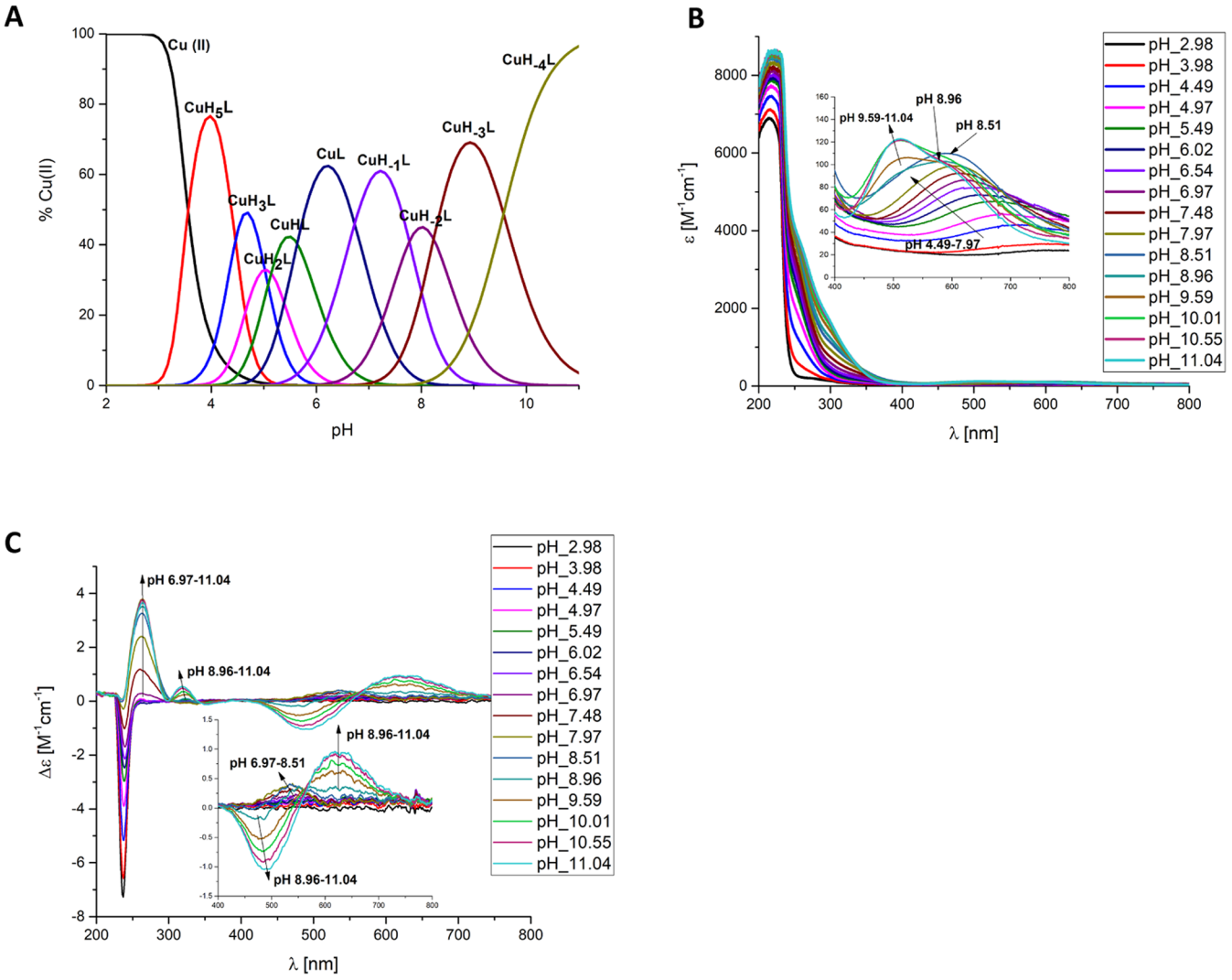

Figure 3. (A) Species distribution diagram, (B) UV−vis absorption spectra, and (C) CD spectra of Cu(II)-Ac-EMMTPHHQDAIDMAE-MALQKAEHPE-NH_2; metal/ligand ratio 1:1; $C_L = 5 \times 10^{-4}$ M. For clarity, the charges on the speciation plot were omitted (see Table 2B).

deprotonation and coordination of the first amide donor (any LMCT $N^- \rightarrow$ Cu(II) bands on CD spectra at pH 6 where $[CuL]^{4-}$ predominates), but at the same time, this pK_a value is rather too low to indicate coordination of the water molecule.[29,46,47] This may suggest that, in the $[CuL]^{4-}$ complex, copper is bound to the two imidazole nitrogen and carboxyl groups of aspartic acid. The involvement of aspartic acid in binding or stabilizing the Cu(II) binding site is further confirmed by NMR studies recorded at pH 7.4 (see the description below). A similar phenomenon was observed in a recently published paper, where the coordination properties of Cu(II) ions toward the peptides Ac-GSTENLKH-NH2 (R1) and Ac-GS(P)TENLKH-NH2 (R1P) (Ser phosphorylated analogue) were studied.[48] The next three species, $[CuH_{-1}L]^{5-}$, $[CuH_{-2}L]^{6-}$, and $[CuH_{-3}L]^{7-}$, result from the copper interaction with the amide group of the peptide chain, forming 3N and 4N complexes. The involvement of an increasing number of nitrogen atoms in Cu(II) binding is proven by a blue shift, 647 → 511 nm, in the UV−vis spectra (Figure 3B and Table 2B). The square-planar $1N_{im}$, $3N^-$ complex appeared at pH 9, as indicated by the typical shape of CD bands in the visible region (positive and negative Cotton effect at λ = 622 nm, $\Delta\varepsilon$ = 0.59 cm^{-1} M^{-1} and λ = 477 nm, $\Delta\varepsilon$ = −0.52 cm^{-1} M^{-1}, respectively) (Figure 3C and Table 2B). The last $[CuH_{-4}L]^{8-}$ species with pK_a = 9.56 results from the deprotonation of a lysine residue, which does not participate in the binding (pK_a = 9.94 for the free ligand) (Table 2B).

NMR analysis indicated that, after the addition of 0.1 equiv of copper to **Ac-$_{51}$EMMTPHHQDAIDMAEMALQKAEHPE$_{75}$-NH_2**, the most affected cross-peaks were those of the histidines, prolines, and Lys70, as shown in the TOCSY spectrum (Figure 4A). The subsequent addition of 0.2 equiv of Cu(II) not only intensified the effects on the previously mentioned residues but also caused further broadening of the correlations associated with Thr55, Asp59, Ile61, and Asp69 (Figure 4B). At the same time, analysis of the 1D spectrum revealed not only the effects on the aromatic proton of the three histidines but also the selective broadening of the methyl groups of methionines (Figure S3). Notably, the singlets corresponding to the $-SCH_3$ groups were affected differently, with two of the four observed signals being more influenced than the others. These results support copper coordination to the three histidines through their imidazole nitrogens (the spectroscopic parameters indicate binding to two His residues at the same time and possible fast exchange with the third residue) and suggest the

https://doi.org/10.1021/acs.inorgchem.4c05101
Inorg. Chem. 2025, 64, 2936−2950

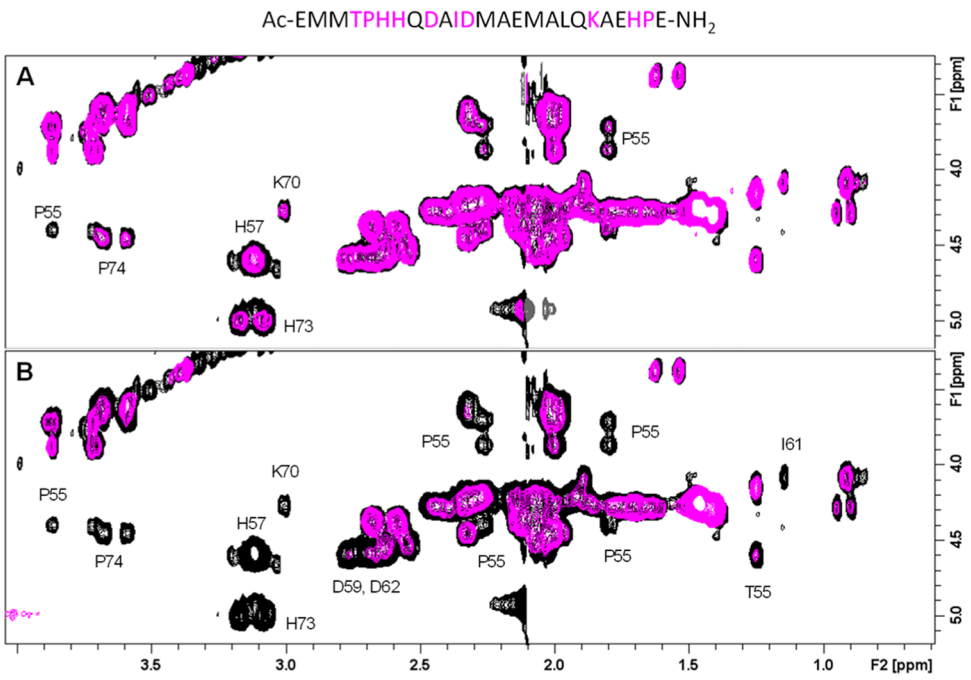

Figure 4. Superimposition of the aliphatic regions of 2D $^{1}H-^{1}H$ TOCSY NMR spectra of Ac-$_{51}$EMMTPHHQDAIDMAEMALQKAEHPE$_{75}$-NH_2 (0.5 mM) in the absence (black) and presence (magenta) of (A) 0.1 and (B) 0.2 Cu(II) equivalents. Spectra were recorded at 288 K in 20 mM phosphate buffer, pH 7.4. The peptide sequence is shown at the top, with the most affected residues highlighted in magenta.

involvement of the carboxyl group of one of the two aspartates in completing the coordination sphere. The involvement of the carboxyl group in the binding of Cu(II) ions in the studied peptide seems to be entirely possible in relation to the literature data describing the binding of Cu(II) ions to two MxxHH motifs of the CopM transporter, where, in addition to two histidine residues (one from each motif), Asp59 also participates in the binding.[15]

To better understand which methionine residues are most affected by the paramagnetic ion and to have a better characterization of the metal coordination sphere, we analyzed the effect of copper on the amide proton correlations by comparing the fingerprint regions of the TOCSY spectrum in the absence and presence of Cu(II) (Figure 5). The data indicate that even after the addition of 0.1 equiv of copper, substantial changes are observed in many of the correlations. In particular, beyond the previously noted effects, broadening is seen in other residues primarily located in the N-terminal (Met52 and Met53) and C-terminal regions (Met66, Glu72, and Glu75). Further addition of 0.2 equiv results in excessive broadening, preventing the extraction of detailed information. Among the methionine residues, the most pronounced effects are observed on Met53 and Met66, both likely being involved in the stabilization of the binding site. In the first case, Met53 may be facilitated by its proximity to the His−His pair. In the second case, Met66 could be located near the binding site due to backbone folding induced by His73 coordinating with the paramagnetic ion.

In the case of the Cu(II) binding site in the CopM metallophore, **Ac-GMMGMHQGHGMMAMD-NH_2** (which contains the MHxxH motif), Cu(II) begins to coordinate to this ligand at a very low pH (Figure 6A). The first detected complex is $[CuH_2L]^{3+}$, where the carboxyl group of the Asp residue present in the peptide sequence may participate in the coordination at acidic pH. Upon an increase in pH, the two histidines with pK_a values of 4.44 and 5.17 undergo

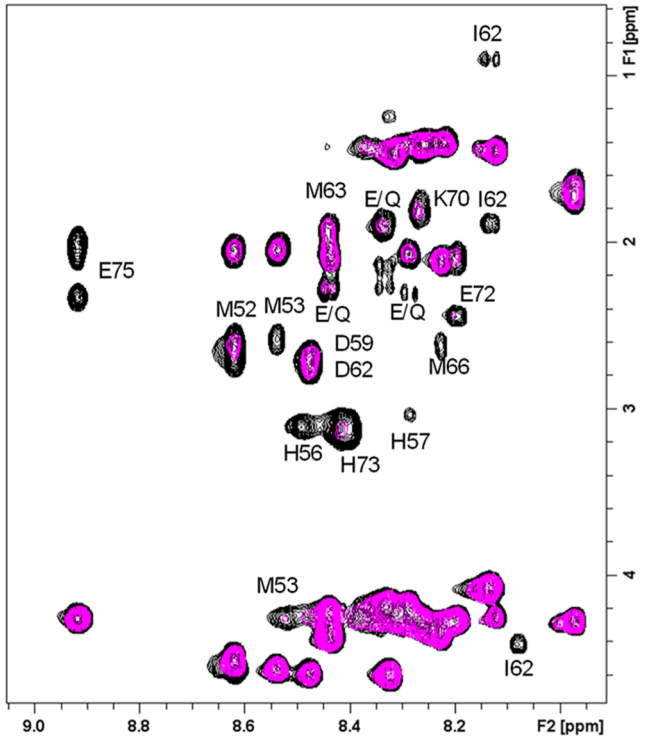

Figure 5. Superimposition of the fingerprint regions of 2D $^{1}H-^{1}H$ TOCSY NMR spectra of Ac-$_{51}$EMMTPHHQDAIDMAEMALQKAEHPE$_{75}$-NH_2 (0.5 mM) in the absence (black) and presence (magenta) of 0.1 Cu(II) equivalents. Spectra were recorded at 288 K in 20 mM phosphate buffer, pH 7.4. The label E/Q refers to correlations that were not unequivocally assigned to Glu or Gln residues.

deprotonation, leading to the formation of the $[CuHL]^{2+}$ and $[CuL]^{+}$ species (Table 2C and Figure 6B). The

https://doi.org/10.1021/acs.inorgchem.4c05101
Inorg. Chem. 2025, 64, 2936−2950

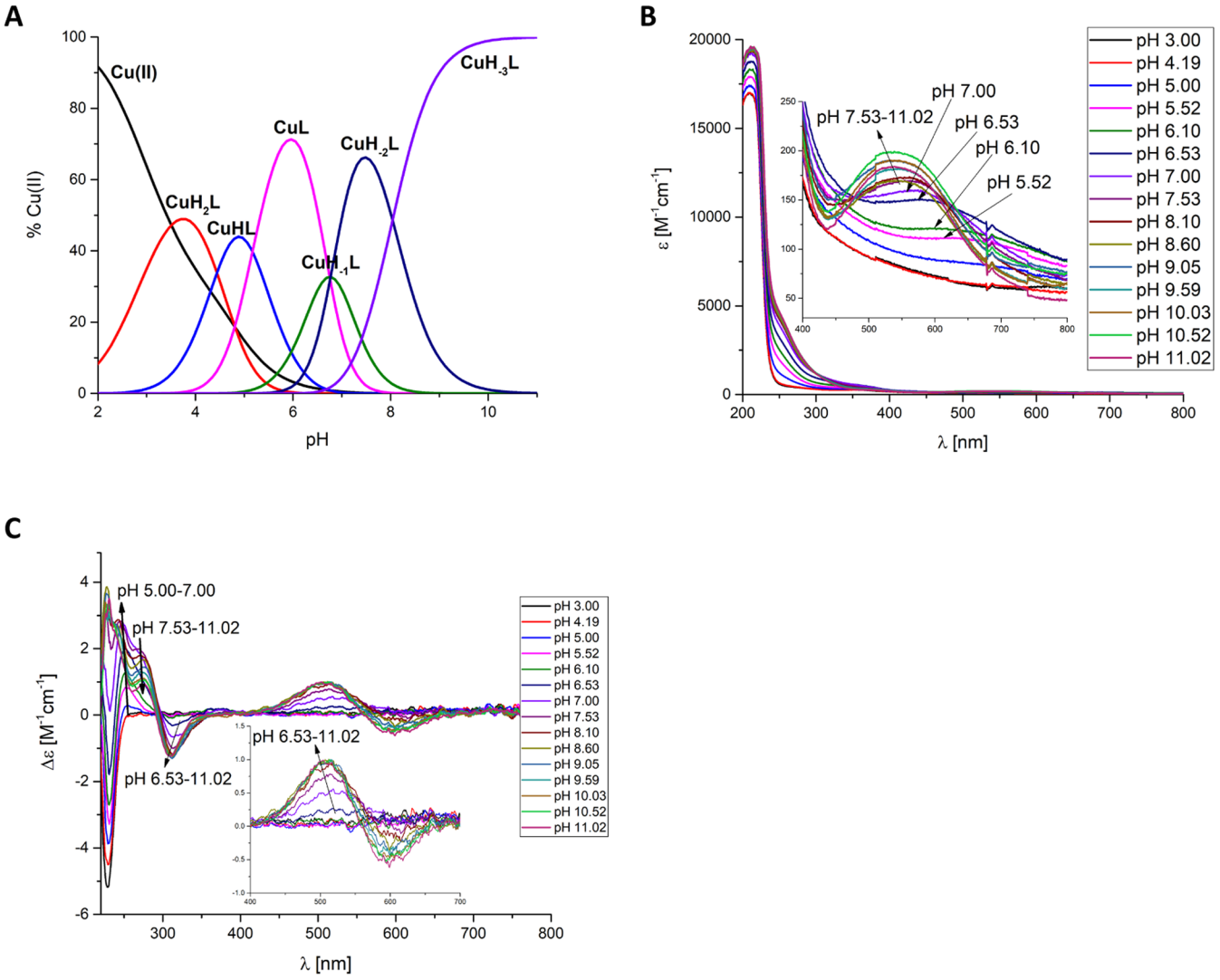

Figure 6. (A) Species distribution diagram, (B) UV−vis absorption spectra, and (C) CD spectra of Cu(II)-Ac-GMMG**MH**QG**H**GMMAMD-NH_2; metal/ligand ratio 1:1; $C_L = 5 \times 10^{-4}$ M. For clarity, the charges on the speciation plot were omitted (see Table 2C).

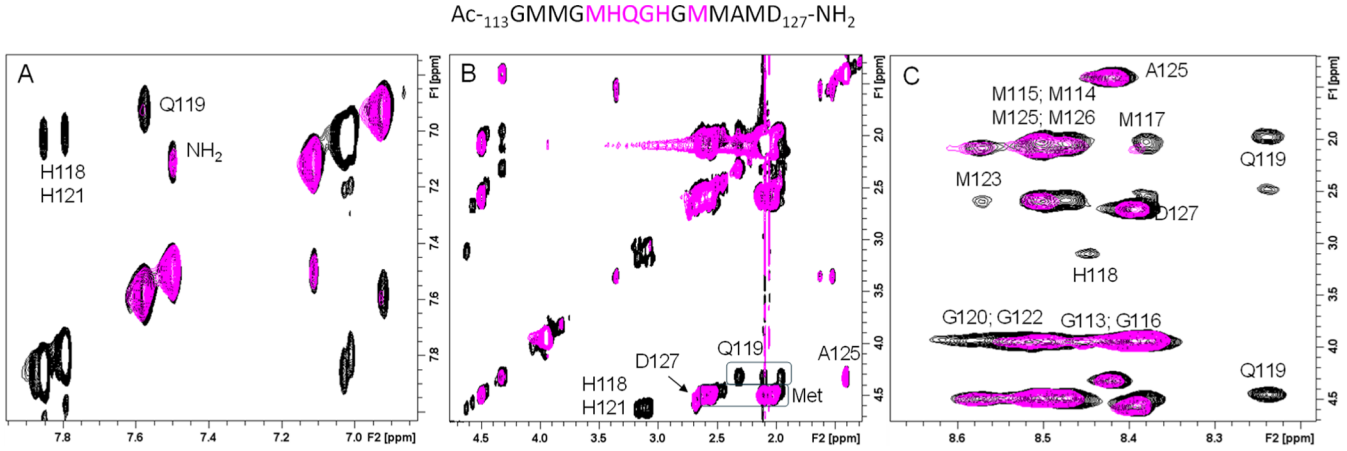

Figure 7. Superimposition of (A) aromatic, (B) aliphatic, and (C) fingerprint regions of 2D $^1H-^1H$ TOCSY NMR spectra of Ac-$_{113}$GMMGMHQGHGMMAMD$_{127}$-NH_2 (0.5 mM) in the absence (black) and presence (magenta) of 0.1 Cu(II) equivalents. Spectra were recorded at 288 K in 20 mM phosphate buffer, pH 7.4. The peptide sequence is shown at the top, with the most affected residues highlighted in magenta.

involvement of imidazole nitrogens of two histidines in Cu(II) binding provides a characteristic charge transfer N_{im}-Cu(II) band present at around 250 nm on the CD spectra (Figure 6C). Moving to alkaline conditions, the CD spectra show an

https://doi.org/10.1021/acs.inorgchem.4c05101
Inorg. Chem. 2025, 64, 2936−2950

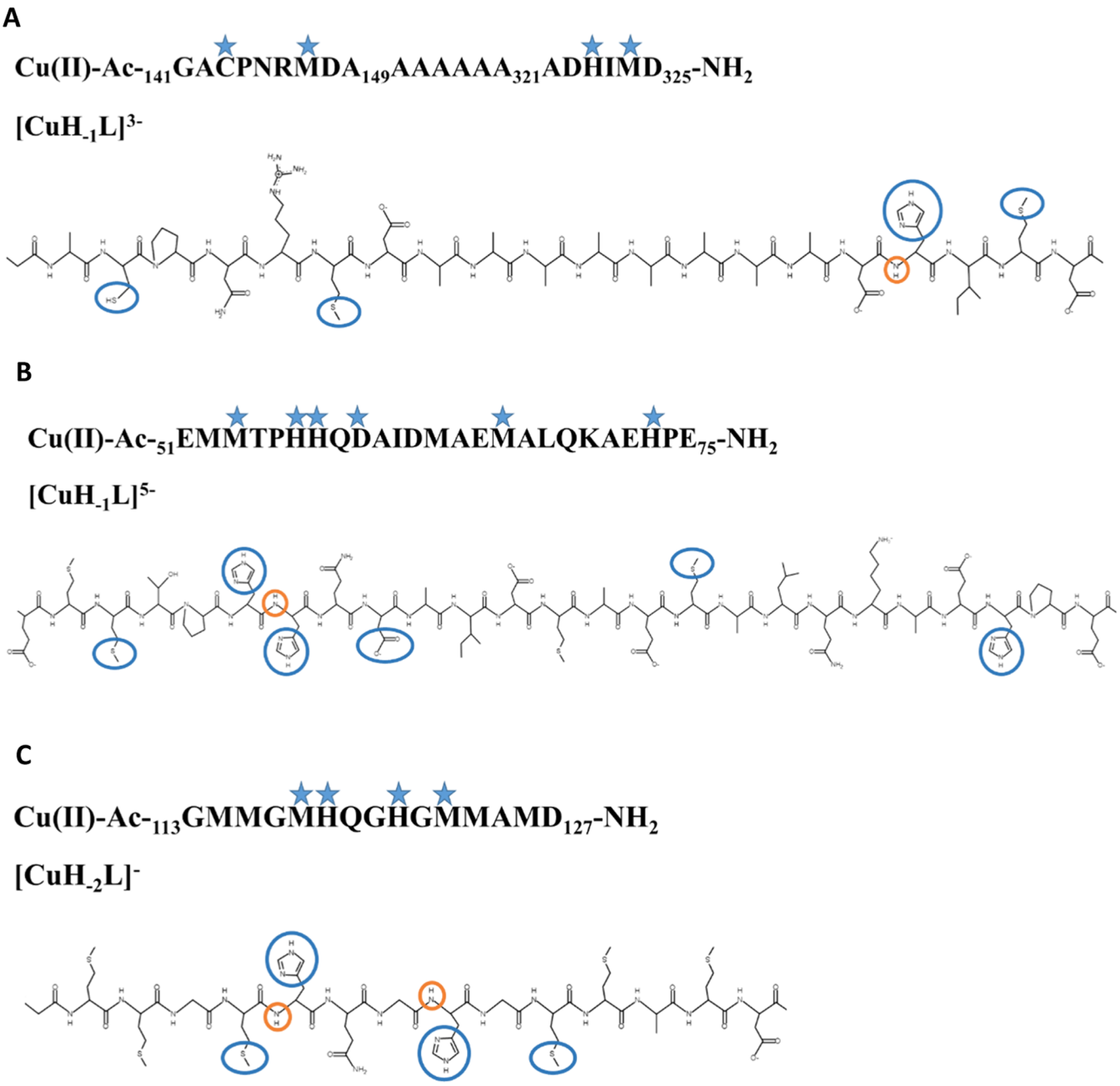

Figure 8. Scheme showing the most probable donor atoms involved in the coordination of Cu(II) ions in (A) OprC CxxxM-HxM domain, (B) CopM MxxHH domain, and (C) CopM MHxxH domain. Side groups of binding amino acids are highlighted with blue circles and potential amide nitrogens of the peptide bond completing the coordination sphere are highlighted with orange circles.

increasing signal in the visible region, which can be ascribed to the backbone amides. The $[CuH_{-1}L]$ species, which reaches its maximum concentration at pH 6.80, comes from deprotonation of the amide nitrogen. In the UV−vis spectrum, the maximum absorption at 574 nm is observed, which supports a three nitrogen $2N_{im}$, $1N^{-}$ binding mode in the coordination sphere of Cu(II) (Figure 6B and Table 2C). Above pH 7.50, where the $[CuH_{-2}L]^{-}$ complex dominates, a UV−vis band with a maximum absorption at 554 nm indicates the formation of a 4N complex (Figure 6B and Table 2C). Additionally, the CD spectrum shows positive and negative Cotton effects at 515 and 605 nm, respectively. These observations indicate the typical square-planar geometry associated with the compound (Figure 6C). The last species, $[CuH_{-3}L]^{2-}$, results from the replacement of one imidazole nitrogen atom by an amide, indicating a $1N_{im}$, $3N^{-}$ set of donors (Table 2C).

The NMR analysis of **Ac-$_{113}$GMMGMHQGHGMMAMD$_{127}$-NH$_2$** was conducted in the same manner as that for the two previous systems. Following the addition of copper, which caused selective variations in the NMR signals, the regions of the 1D and 2D spectra most affected by the paramagnetic ion were identified. The 1D spectrum once again revealed broadening of the aromatic signals of the histidines along with selective broadening of some thioether group signals from the six methionine residues (Figure S4). At the same time, the analysis of the 2D $^{1}H-^{1}H$ TOCSY maps confirmed the effects on His118 and H121 highlighting the broadening of Gln119 and

https://doi.org/10.1021/acs.inorgchem.4c05101
Inorg. Chem. 2025, 64, 2936−2950

Gly120, located between the histidine residues, along with variations in the cross-peaks of Met117 and Met123 (Figure 7). These findings strongly suggest Cu(II) binding to both the imidazole nitrogens of the histidine and the thioether groups of Met117 and Met123.

Taking into account the potentiometric and spectroscopic (UV−vis, CD, EPR, and NMR) studies, the most probable donor groups of the OprC and CopM complex species dominating at pH 7.4 are presented in Figure 8.

Can Cu(II) Coordination Affect the Structures of OprC and CopM Domains? In order to have very basic information about structural properties of investigated ligands and their Cu(II) complexes, far-UV CD spectroscopy was used to monitor the structural changes after adding metal in the pH range 3−11 (Figure S5). Although the addition of the copper ions does not change the structure of the investigated ligands, the CD spectra for the apo forms, in particular, OprC and CopM MxxHH metal-binding domains, seem very interesting (Figure S5A,B). At acidic pH, both ligands adopt an α helical structure. In the case of Ac-EM**M**TP**HH**QDAIDMAEMALQKAEHPE-NH_2, the clearly outlined two negative absorption bands at 205 and 225 nm (Figure S5B) indicate an even higher percentage of the α helical structure than in the case of the OprC domain (Figure S5A). For both ligands, as the pH value increases, the spectrum shows a shift toward shorter wavelengths (205 → 200 nm, hypsochromic effect) and a decrease in the intensity of the negative band at around 225 nm. This indicates a tendency for the structure to change from α-helical to disordered in increasing pH values. The change in the structure with increasing pH is probably related to the change in the charge of the peptides, indicating the deprotonation of the side chains of amino acids present in the sequences (Asp, Glu, His, Cys, and Lys). The CopM MHxxH domain and its Cu(II) complexes on CD spectra show a strong negative absorption band at 197 nm, confirming a random coil structure in all pH ranges regardless of the presence or absence of Cu(II) (Figure S5C).

Comparison of the Thermodynamic Stability of an Unprecedented CxxxM-HxM Metal-Binding Site of OprC with Two MxxHH and MHxxH Motifs of CopM. There is a significant difference in the efficiency of metal-binding between the OprC and CopM domains, as visualized on the competition plot, based on the potentiometric stability constants, which simulates a hypothetical situation in which equal amounts of Cu(II) and the studied peptides are present in solution. Above pH 4, the CopM MxxHH metal-binding domain is a much more efficient Cu(II) binder than its MHxxH metal-binding domain and CxxxM-HxM metal-binding site of OprC (Figure 9). At pH 7.4, which is the most interesting (physiological) value in most biological systems, almost 100% of the available Cu(II) would be bound to Ac-EM**M**TP**HH**QDAIDMAEMALQKAEHPE-NH_2 (CopM MxxHH metal-binding domain). In our hypothetical simulation, the CopM MHxxH metal-binding domain and CxxxM-HxM metal-binding site of the transmembrane OprC have no chance in competition with the Ac-EM**M**TP**HH**QDAIDMAEMALQKAEHPE-NH_2 fragment. It seems that the CopM MxxHH motif, where two coordinating histidine residues are localized next to each other, is much more effective in Cu(II) binding than the CopM MHxxH motif where two binding histidines are separated by two other amino acid residues. Moreover, the CxxxM-HxM metal-binding site of OprC, where, in addition to histidine, cysteine residue may

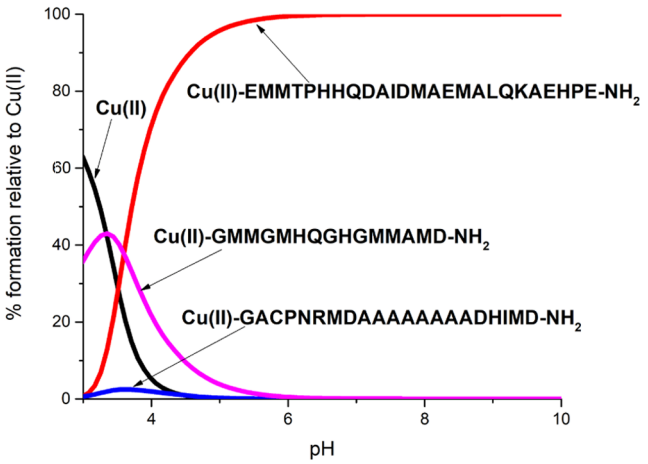

Figure 9. Competition plots for the Cu(II) complexes with Ac-GACPNRMDAAAAAAAADHIMD-NH_2 (CxxxM-HxM metal-binding site of OprC), Ac-EMMTPHHQDAIDMAEMALQKAEHPE-NH_2 (CopM MxxHH metal-binding domain), and Ac-GMMGMHQGHGMMAMD-NH_2 (CopM MHxxH metal-binding domain) based on potentiometric data (Tables 1 and 2).

also bind Cu(II) ions, does not constitute any competition in Cu(II) binding for the CopM MxxHH domain. The obtained comparison may suggest that the CopM metallophore (more precisely, its MxxHH binding site) binds Cu(II) ions very strongly and is unable to give them back to the OprC transmembrane transporter; therefore, it is perhaps transported together with copper ions through OprC into the bacterial cell.

To better understand the interaction between OprC and CopM protein (in particular, its CopM MxxHH domain, which forms the most stable Cu(II) complexes; see Figure 9), the ITC measurements were a perfect method of choice. ITC provides conditional results, which perfectly compare the findings for all three peptides, as the measurements were performed under precisely the same conditions. The best-fit values for stoichiometry (n_{ITC}), stability constant ($K_{d\ ITC}$), and change in enthalpy (ΔH_{ITC}) were determined by using a one-site binding model. All three peptides exhibit moderate affinities for Cu(II) binding, with the Ac-EM**M**TP**HH**QDAIDMAEMALQKAEHPE-NH_2 peptide displaying the highest affinity, which is consistent with our potentiometric results. The OprC Ac-GA**C**PNR**M**DAAAAAAAAD**HIM**D-NH_2 peptide's binding to Cu(II) is primarily driven by a net favorable change in entropy. Both CopM binding sites, the Ac-EM**M**TP**HH**QDAIDMAEMALQKAEHPE-NH_2 and Ac-GMMG**MH**QG**H**GMMAMD-NH_2 peptides, exhibit a biphasic binding pattern to Cu(II) ions at this pH (Figure 10). In contrast to the CxxxM-HxM binding domain of OprC, these two peptides may exhibit an M/L 1:2 stoichiometry, indicating that two CopM domains can form bis-complexes. This observation aligns with our previous findings involving poly-His and poly-Asp peptides, which were titrated with metal ions at a specific pH.[43,49] However, we emphasize here that the formation of complexes with stoichiometry other than M/L 1:1 was not confirmed by MS and potentiometric studies. Several factors could explain the formation of M/L 1:2 complexes in ITC. Most probably, when a peptide is titrated into a solution of metal ions, the peptide concentration is much lower, which can lead to a different interaction profile. The saturation of binding sites may occur more slowly in this reversed titration, and the thermodynamics could differ due to

https://doi.org/10.1021/acs.inorgchem.4c05101
Inorg. Chem. 2025, 64, 2936−2950

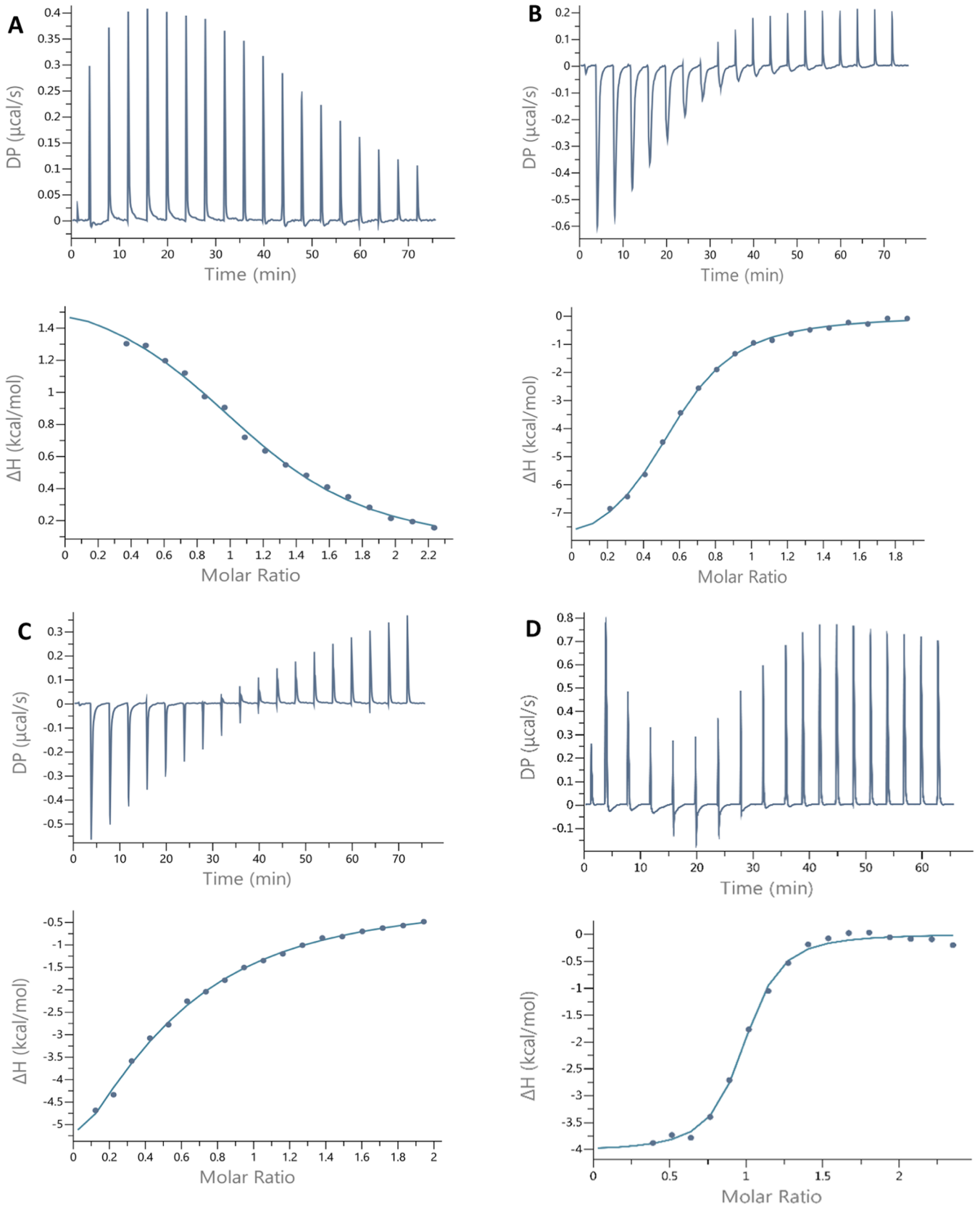

Figure 10. Representative ITC data (above) and their corresponding thermodynamic signatures (below) for Cu(II) (1.0−2.0 mM) titrated into (A) Ac-GACPNRMDAAAAAAAADHIMD-NH_2, (B) Ac-EMMTPHHQDAIDMAEMALQKAEHPE-NH_2, and (C) Ac-GMMGMHQGHGMMAMD-NH_2 peptides (100−200 μM) at pH 7.0. (D) Representative ITC data for the reverse titration (1 mM Ac-EMMTPHHQDAIDMAEMALQKAEHPE-NH_2 peptide to 100 μM Cu(II)), pH 7.0.

https://doi.org/10.1021/acs.inorgchem.4c05101
Inorg. Chem. 2025, 64, 2936−2950

Table 3. Experimental Thermodynamic Values for Cu(II) Binding to Ac-GACPNRMDAAAAAAAADHIMD-NH_2 (GAC), Ac-GMMGMHQGHGMMAMD-NH_2 (GMM), and Ac-EMMTPHHQDAIDMAEMALQKAEHPE-NH_2 (EMM) from ITC Measurements in 25 mM Caco Buffer, pH 7.0 at 25 °C

	GAC	GMM	EMM	EMM(r)
$K_{d\,ITC}$ [μM]	34.0 ± 11.7	97.0 ± 25.00	14.0 ± 1.05	1.48 ± 0.282
ΔH_{ITC} [kcal/mol]	1.59 ± 0.20	−11.0 ± 2.49	−8.58 ± 0.199	−4.05 ± 0.11
n_{ITC}	1.01 ± 0.047	0.452 ± 0.050	0.557 ± 0.006	0.940 ± 0.011
$-T\Delta S_{ITC}$ [kcal/mol]	−7.69	5.54	1.96	−3.91

the changed molar ratios. The system's response can vary significantly depending on whether metal ions are the limiting factor (as in the first case) or whether the peptide is at a lower concentration (as in the reverse titration). Additionally, for peptides with multiple charged residues, the peptide may initially interact with the metal in a less ordered manner compared to when metal ions are the limiting reagent and the peptide is more likely to form stable complexes. The way charged residues on the peptide (such as histidines and aspartates) interact with Cu(II) ions can lead to different entropic and enthalpic contributions. Moreover, when titrating the peptide into the metal ion solution, the relative arrangement of charges may change, and the overall complexity of binding could cause entropic contributions to become more significant, which might explain the observed differences in the thermodynamic behavior.

Reversing the titration direction (adding the peptide to the Cu(II) solution) reveals a 1:1 binding for Ac-EM**M**TP**HH**Q-DAIDMAEMALQKAEHPE-NH_2 peptide (Figure 10D and Table 3). This data were also fit to a single-site binding model. The reversed titration indicates an even higher affinity of the Ac-EM**M**TP**HH**QDAIDMAEMALQKAEHPE-NH_2 peptide for Cu(II) (Table 3). To further investigate this, we performed ITC titrations to study the competition for Cu(II) ions between Ac-EM**M**TP**HH**QDAIDMAEMALQKAEHPE-NH_2 and Ac-GA**C**PNR**M**DAAAAAAAAD**HIM**D-NH_2 peptides. The results showed an affinity of 8.32 ± 0.9 μM when Ac-EM**M**TP**HH**QDAIDMAEMALQKAEHPE-NH_2 was titrated into Ac-GA**C**PNR**M**DAAAAAAAAD**HIM**D-NH_2 pretreated with Cu(II) in a 1:1 ratio (Figure S6A). In contrast, when Ac-GA**C**PNR**M**DAAAAAAAAD**HIM**D-NH_2 was titrated into Ac-EM**M**TP**HH**QDAIDMAEMALQKAEHPE-NH_2 pretreated with Cu(II), the DP change was too weak to fit the data to any model and calculate meaningful results (Figure S6B).

CONCLUSIONS

In this work, we wanted to find out if it was thermodynamically possible for the CopM metallophore to pass over Cu(II) to the OprC transmembrane protein. In order to find this, we analyzed Cu(II) complexes of a novel **CxxxM-HxM** metal-binding site from the OprC transmembrane protein (Ac-GA**C**PNR**M**DAAAAAAAAD**HIM**D-NH_2) and two metal-binding sites of the putative CopM metallophore (Ac-EM**M**TP**HH**QDAIDMAEMALQKAEHPE-NH_2 and Ac-GMMG**MH**QG**H**GMMAMD-NH_2).

All examined complexes exist in equimolar stoichiometry. The spectroscopic and potentiometric studies reveal that the OprC peptide fragment involves Cys143 and His323 in Cu(II) binding, with possible contributions from Met-SCH_3 groups in the metal coordination sphere. The methyl protons of both methionine residues, located close to Cys and His, are significantly affected by the presence of a paramagnetic ion. In the MxxHH metal-binding domain of CopM (Ac-EM**M**TP**HH**QDAIDMAEMALQKAEHPE-NH_2), two of the three imidazole groups of histidine residues bind Cu(II); however, both potentiometric and NMR studies indicate a dynamic exchange involving all three histidines present in the sequence. Additionally, broadening of the NMR signals from two methionyl groups (of the four present in the sequence) may suggest the coordination of these groups in an axial position, completing the Cu(II) binding sphere at pH 7. Moreover, NMR studies confirm the involvement of one Asp in Cu(II) binding. In the MHxxH metal-binding domain of CopM (Ac-GMMG**MH**QG**H**GMMAMD-NH_2), which has a significantly lower affinity for Cu(II) compared to the CopM MxxHH domain, Cu(II) ions bind to two histidyl residues and two of the six methionine thioether groups, located closest to two imidazoles.

The potentiometric and ITC results clearly show a significant difference in the efficiency of metal-binding between the OprC and the CopM domains. At pH 7, the metal-binding site of CopM with the MxxHH motif is the most effective ligand for Cu(II) ions compared to the MHxxH binding site of CopM and the novel CxxxM-HxM metal-binding site from OprC. This finding confirms that two adjacent histidine residues are much more effective in Cu(II) binding than two imidazoles separated by two other amino acid residues. Moreover, the CxxxM-HxM metal-binding site in OprC, where a cysteine residue also binds Cu(II) ions alongside histidine, does not compete effectively for Cu(II) with the MxxHH CopM metal-binding site. This comparison suggests that the MxxHH domain of the CopM metallophore binds Cu(II) ions very strongly and may retain them during transport through OprC, potentially facilitating the passage of both the CopM metallophore and bound copper ions into the bacterial cell.

The obtained results, suggesting a potential interaction between the CopM metallophore fragment and the transmembrane protein OprC in vitro, could initiate highly valuable *in vivo* studies to track and understand the mechanism of copper ion transport by bacteria. Additionally, the potential attachment of an antibiotic to the CopM metallophore fragment, recognized by OprC (Trojan horse strategy), could contribute to the development of new treatment strategies, which is crucial in the era of rapidly advancing antibiotic resistance.

ASSOCIATED CONTENT

Supporting Information

The Supporting Information is available free of charge at https://pubs.acs.org/doi/10.1021/acs.inorgchem.4c05101.

Mass spectra and m/z values for Cu(II)-peptide systems; EPR spectra for Cu(II)-peptides; 1H NMR spectra for CopM domains and their Cu(II) complexes; far-UV CD spectra for CopM and OprC domains and its Cu(II)

https://doi.org/10.1021/acs.inorgchem.4c05101
Inorg. Chem. 2025, 64, 2936−2950

complexes; and ITC titrations to study the competition for Cu(II) ions between CopM and OprC fragments (Figures S1−S6, Table S1) (PDF)

AUTHOR INFORMATION

Corresponding Author

Aleksandra Hecel − *Faculty of Chemistry, University of Wroclaw, 50-383 Wroclaw, Poland;* orcid.org/0000-0002-4314-9599; Email: aleksandra.hecel2@uwr.edu.pl

Authors

Arian Kola − *Department of Biotechnology, Chemistry and Pharmacy, University of Siena, 53100 Siena, Italy*

Daniela Valensin − *Department of Biotechnology, Chemistry and Pharmacy, University of Siena, 53100 Siena, Italy*

Danuta Witkowska − *Institute of Health Sciences, University of Opole, 45-060 Opole, Poland*

Complete contact information is available at: https://pubs.acs.org/10.1021/acs.inorgchem.4c05101

Notes

The authors declare no competing financial interest.

ACKNOWLEDGMENTS

The work was supported by the National Science Centre (Grant UMO-2023/51/D/ST5/01798), the Polish National Agency for Academic Exchange (Grant BPN/BKK/2022/1/00005), and the Excellence Initiative—Research University Grant BPIDUB.13.2024.

REFERENCES

(1) Samanovic, M.; Ding, C.; Thiele, D.; Darwin, K. Copper in Microbial Pathogenesis: Meddling with the Metal. *Cell Host Microbe* **2012**, *11* (2), 106−115.

(2) Darwin, K. H. Mycobacterium tuberculosis and Copper: A Newly Appreciated Defense against an Old Foe? *J. Biol. Chem.* **2015**, *290* (31), 18962−18966.

(3) Ekici, S.; Yang, H.; Koch, H.; Daldal, F. Novel Transporter Required for Biogenesis of cbb 3 -Type Cytochrome c Oxidase in *Rhodobacter capsulatus*. *mBio* **2012**, *3* (1), No. e00293-11, DOI: 10.1128/mBio.00293-11.

(4) Banci, L.; Bertini, I.; Cantini, F.; Ciofi-Baffoni, S. Cellular copper distribution: a mechanistic systems biology approach. *Cell. Mol. Life Sci.* **2010**, *67* (15), 2563−2589.

(5) Weiss, G.; Carver, P. Role of divalent metals in infectious disease susceptibility and outcome. *Clin. Microbiol. Infect.* **2018**, *24* (1), 16−23.

(6) Andrei, A.; Öztürk, Y.; Khalfaoui-Hassani, B.; Rauch, J.; Marckmann, D.; Trasnea, P.; Daldal, F.; Koch, H. Cu Homeostasis in Bacteria: The Ins and Outs. *Membranes* **2020**, *10* (9), No. 242.

(7) Hofmann, L.; Hirsch, M.; Ruthstein, S. Advances in Understanding of the Copper Homeostasis in *Pseudomonas aeruginosa*. *Int. J. Mol. Sci.* **2021**, *22* (4), No. 2050.

(8) Khalfaoui-Hassani, B.; Wu, H.; Blaby-Haas, C.; Zhang, Y.; Sandri, F.; Verissimo, A.; Koch, H.; Daldal, F. Widespread Distribution and Functional Specificity of the Copper Importer CcoA: Distinct Cu Uptake Routes for Bacterial Cytochrome c Oxidases. *mBio* **2018**, *9* (1), No. e00065-18, DOI: 10.1128/mBio.00065-18.

(9) Quintana, J.; Novoa-Aponte, L.; Argüello, J. Copper homeostasis networks in the bacterium *Pseudomonas aeruginosa*. *J. Biol. Chem.* **2017**, *292* (38), 15691−15704.

(10) Saier, M. H.; Chauvaux, S.; Cook, G.; Deutscher, J.; Paulsen, I.; Reizer, J.; Ye, J. Catabolite repression and inducer control in Gram-positive bacteria. *Microbiology* **1996**, *142*, 217−230.

(11) Lima, S.; Matinha-Cardoso, J.; Giner-Lamia, J.; Couto, N.; Pacheco, C.; Florencio, F.; Wright, P.; Tamagnini, P.; Oliveira, P. Extracellular vesicles as an alternative copper-secretion mechanism in bacteria. *J. Hazard. Mater.* **2022**, *431*, No. 128594.

(12) Bhamidimarri, S. P.; Young, T.; Shanmugam, M.; Soderholm, S.; Basle, A.; Bumann, D.; van den Berg, B. Acquisition of ionic copper by the bacterial outer membrane protein OprC through a novel binding site. *PLoS Biol.* **2021**, *19* (11), No. e3001446, DOI: 10.1371/journal.pbio.3001446.

(13) Gao, P.; Guo, K.; Pu, Q.; Wang, Z.; Lin, P.; Qin, S.; Khan, N.; Hur, J.; Liang, H.; Wu, M. oprC Impairs Host Defense by Increasing the Quorum-Sensing-Mediated Virulence of *Pseudomonas aeruginosa*. *Front. Immunol.* **2020**, *11*, No. 1696, DOI: 10.3389/fimmu.2020.01696.

(14) Giner-Lamia, J.; López-Maury, L.; Florencio, F. CopM is a novel copper-binding protein involved in copper resistance in Synechocystis sp PCC 6803. *MicrobiologyOpen* **2015**, *4* (1), 167−185.

(15) Zhao, S.; Wang, X.; Niu, G.; Dong, W.; Wang, J.; Fang, Y.; Lin, Y.; Liu, L. Structural basis for copper/silver binding by the Synechocystis metallochaperone CopM. *Acta Crystallogr., Sect. D: Struct. Biol.* **2016**, *72*, 997−1005.

(16) Yang, J.; Gao, M.; Wang, J.; He, C.; Wang, X.; Liu, L. Structural basis of copper binding by a dimeric periplasmic protein forming a six-helical bundle. *J. Inorg. Biochem.* **2022**, *229*, No. 111728.

(17) Gans, P.; O'Sullivan, B. GLEE, a new computer program for glass electrode calibration. *Talanta* **2000**, *51* (1), 33−37.

(18) Gans, P.; Sabatini, A.; Vacca, A. Investigation of equilibria in solution. Determination of equilibrium constants with the HYPERQUAD suite of programs. *Talanta* **1996**, *43* (10), 1739−1753.

(19) Alderighi, L.; Gans, P.; Ienco, A.; Peters, D.; Sabatini, A.; Vacca, A. Hyperquad simulation and speciation (HySS): a utility program for the investigation of equilibria involving soluble and partially soluble species. *Coord. Chem. Rev.* **1999**, *184*, 311−318.

(20) Hwang, T. L.; Shaka, A. J. Multiple-pulse mixing sequences that selectively enhance chemical exchange or cross-relaxation peaks in high-resolution NMR spectra. *J. Magn. Reson.* **1998**, *135* (2), 280−287.

(21) Johnson, R. A.; Manley, O.; Spuches, A.; Grossoehme, N. Dissecting ITC data of metal ions binding to ligands and proteins. *Biochim. Biophys. Acta, Gen. Subj.* **2016**, *1860* (5), 892−901.

(22) Pettit, L. D.; Gregor, J. E.; Kozłowski, H. Complex Formation between Metal Ions and Peptides. In *Perspectives on Bioinorganic Chemistry*; Hay, R. W.; Dilworth, J. R.; Nolan, K. B., Eds.; JAI Press: London, 1991; Vol. *1*, pp 1−41.

(23) Hecel, A.; Garstka, K.; Kozloeski, H.; Rowinska-Zyrek, M. -HH and -HAAAH motifs act as fishing nets for biologically relevant metal ions in metallopeptides. *J. Inorg. Biochem.* **2024**, *252*, No. 112456, DOI: 10.1016/j.jinorgbio.2023.112456.

(24) Krzywoszyńska, K.; Swiatek-Kozlowska, J.; Potocki, S.; Ostrowska, M.; Kozlowski, H. Triplet of cysteines - Coordinational riddle? *J. Inorg. Biochem.* **2020**, *204*, No. 110957.

(25) Witkowska, D.; Rowinska-Zyrek, M.; Valensin, G.; Kozlowski, H. Specific poly-histidyl and poly-cysteil protein sites involved in Ni2+ homeostasis in Helicobacter pylori. Impact of Bi3+ ions on Ni2+ binding to proteins. Structural and thermodynamic aspects. *Coord. Chem. Rev.* **2012**, *256* (1−2), 133−148.

(26) Hecel, A.; Watly, J.; Rowinska-Zyrek, M.; Swiatek-Kozlowska, J.; Kozlowski, H. Histidine tracts in human transcription factors: insight into metal ion coordination ability. *JBIC, J. Biol. Inorg. Chem.* **2018**, *23* (1), 81−90.

(27) Prenesti, E.; Daniele, P.; Prencipe, M.; Ostacoli, G. Spectrum-structure correlation for visible absorption spectra of copper(II) complexes in aqueous solution. *Polyhedron* **1999**, *18* (25), 3233−3241.

(28) Lesiów, M. K.; Pietrzyk, P.; Bienko, A.; Kowalik-Jankowska, T. Stability of Cu(ii) complexes with FomA protein fragments containing two His residues in the peptide chain. *Metallomics* **2019**, *11* (9), 1518−1531.

(29) Sigel, H.; Martin, R. B. Coordinating properties of the amide bond - stability and structure of metal-ion complexes of peptides and related ligands. *Chem. Rev.* **1982**, *82* (4), 385−426.
(30) Hanaki, A.; Saito, M.; Ikota, N. Copper(II) transport from a leucine-containing tripeptide to cysteine - relationship between the position of isobutyl side-chain in the peptide and the rate of ligand-exchange. *Nippon Kagaku Kaishi* **1995**, No. 5, 388−393.
(31) Hanaki, A.; Ikota, N.; Ueda, J.; Ozawa, T.; Odani, A. Transport of the Cu(II) bound with histidine-containing tripeptides to cysteine. Coordination mode and exchangeability of Cu(II) in the complexes. *Bull. Chem. Soc. Jpn.* **2003**, *76* (11), 2143−2150.
(32) Karavelas, T.; Mylonas, M.; Malandrinos, G.; Plakatouras, J.; Hadjiliadis, N.; Mlynarz, P.; Kozlowski, H. Coordination properties of Cu(II) and Ni(II) ions towards the C-terminal peptide fragment -ELAKHA- of histone H2B. *J. Inorg. Biochem.* **2005**, *99* (2), 606−615.
(33) Zoroddu, M. A.; Kowalik-Jankowska, T.; Kozlowski, H.; Salnikow, K.; Costa, M. Ni(II) and Cu(II) binding with a 14-aminoacid sequence of Cap43 protein, TRSRSHTSEGTRSR. *J. Inorg. Biochem.* **2001**, *84* (1−2), 47−54.
(34) Magrì, A.; Munzone, A.; Peana, M.; Medici, S.; Zoroddu, M.; Hansson, O.; Satriano, C.; Rizzarelli, E.; La Mendola, D. Coordination Environment of Cu(II) Ions Bound to N-Terminal Peptide Fragments of Angiogenin Protein. *Int. J. Mol. Sci.* **2016**, *17* (8), No. 1240.
(35) Farkas, E.; Sovago, I.; Kiss, T.; Gergely, A. Studies on transition-metal peptide complexes. 9. Copper(II) complexes of tripeptides containing histidine. *J. Chem. Soc., Dalton Trans.* **1984**, No. 4, 611−614.
(36) Várnagy, K.; Boka, B.; Sovago, I.; Sanna, D.; Marras, P.; Micera, G. Potentiometric and spectroscopic studies on the copper(II) and nickel(II) complexes of tripeptides of methionine. *Inorg. Chim. Acta* **1998**, *275*−*276* (1−2), 440−446.
(37) Stanila, A.; Marcu, A.; Rusu, D.; Rusu, M.; David, L. Spectroscopic studies of some copper(II) complexes with amino acids. *J. Mol. Struct.* **2007**, *834*−*836*, 364−368.
(38) Jiang, J.; Abramavicius, D.; Bulheller, B.; Hirst, J.; Mukamel, S. Ultraviolet Spectroscopy of Protein Backbone Transitions in Aqueous Solution: Combined QM and MM Simulations. *J. Phys. Chem. B* **2010**, *114* (24), 8270−8277.
(39) De Ricco, R.; Potocki, S.; Kozlowski, H.; Valensin, D. NMR investigations of metal interactions with unstructured soluble protein domains. *Coord. Chem. Rev.* **2014**, *269*, 1−12.
(40) Kola, A.; Hecel, A.; Lamponi, S.; Valensin, D. Novel Perspective on Alzheimer's Disease Treatment: Rosmarinic Acid Molecular Interplay with Copper(II) and Amyloid beta. *Life* **2020**, *10* (7), No. 118.
(41) Kola, A.; Vigni, G.; Valensin, D. Exploration of Lycorine and Copper(II)'s Association with the N-Terminal Domain of Amyloid β. *Inorganics* **2023**, *11* (11), No. 443.
(42) Dudek, D.; Miller, A.; Hecel, A.; Kola, A.; Valensin, D.; Mikolajczyk, A.; Barcelo-Oliver, M.; Matera-Witkiewicz, A.; Rowinnska-Zyrek, M. Semenogelins Armed in Zn(II) and Cu(II): May Bioinorganic Chemistry Help Nature to Cope with Enterococcus faecalis? *Inorg. Chem.* **2023**, *62* (34), 14103−14115.
(43) Miller, A.; Matera-Witkiewicz, A.; Mikolajczyk, A.; Watly, J.; Wilcox, D.; Witkowska, D.; Rowinska-Zyrek, M. Zn-Enhanced Asp-Rich Antimicrobial Peptides: N-Terminal Coordination by Zn(II) and Cu(II), Which Distinguishes Cu(II) Binding to Different Peptides. *Int. J. Mol. Sci.* **2021**, *22* (13), No. 6971.
(44) Pelucelli, A.; Peana, M.; Orzel, B.; Piasta, K.; Gumienna-Kontecka, E.; Medici, S.; Zoroddu, M. Zn2+ and Cu2+ Interaction with the Recognition Interface of ACE2 for SARS-CoV-2 Spike Protein. *Int. J. Mol. Sci.* **2023**, *24* (11), No. 9202, DOI: 10.3390/ijms24119202.
(45) Kállay, C.; Várnagy, K.; Micera, G.; Sanna, D.; Sóvágó, I. Copper(II) complexes of oligopeptides containing aspartyl and glutamyl residues.: Potentiometric and spectroscopic studies. *J. Inorg. Biochem.* **2005**, *99* (7), 1514−1525.
(46) Jakab, N. I.; Jancsó, A.; Gajda, T.; Gyurcsik, B.; Rockenbauer, A. Copper(II), nickel(II) and zinc(II) complexes of N-acetyl-His-Pro-His-His-NH2: Equilibria, solution structure and enzyme mimicking. *J. Inorg. Biochem.* **2008**, *102* (7), 1438−1448.
(47) Kamińska, J.; Hecel, A.; Slowik, J.; Rombel-Bryzek, A.; Rowinska-Zyrek, M.; Witkowska, D. Characterization of four peptides from milk fermented with kombucha cultures and their metal complexes-in search of new biotherapeutics. *Front. Mol. Biosci.* **2024**, *11*, No. 1366588, DOI: 10.3389/fmolb.2024.1366588.
(48) Kyriakou, D.; Bletsa, E.; Moussis, V.; Deligiannakis, Y.; Malandrinos, G. Coordination properties of Cu(ii) ions towards a phosphorylated fragment from the R1 domain of the tau protein and the effect of Ser phosphorylation on Cu(ii) binding affinity. *Dalton Trans.* **2022**, *52* (1), 58−69.
(49) Witkowska, D.; Szebesczyk, A.; Watly, J.; Braczkowski, M.; Rowinska-Zyrek, M. A Comparative Study on Nickel Binding to Hpn-like Polypeptides from Two Helicobacter pylori Strains. *Int. J. Mol. Sci.* **2021**, *22* (24), No. 13210.

https://doi.org/10.1021/acs.inorgchem.4c05101
Inorg. Chem. 2025, 64, 2936−2950